



Biological and climate factors co-regulated spatial-temporal dynamics of vegetation autumn phenology on the Tibetan Plateau



Jiaxing Zu^{a,b}, Yangjian Zhang^{a,b,c,*}, Ke Huang^a, Yaojie Liu^{a,b}, Ning Chen^{a,b}, Nan Cong^a

^a Key Laboratory of Ecosystem Network Observation and Modeling, Institute of Geographic Sciences and Natural Resources Research, Chinese Academy of Sciences, Beijing, China

^b College of Resources and Environment, University of Chinese Academy of Sciences, Beijing, China

^c Center for Excellence in Tibetan Plateau Earth Sciences, Chinese Academy of Sciences, Beijing, China

ARTICLE INFO

Keywords:

Vegetation phenology
Tibetan Plateau
End of season (EOS)
Climate change
BRT model

ABSTRACT

Climate change is receiving mounting attentions from various fields and phenology is a commonly used indicator signaling vegetation responses to climate change. Previous phenology studies have mostly focused on vegetation greening-up and its climatic driving factors, while autumn phenology has been barely touched upon. In this study, vegetation phenological metrics were extracted from MODIS NDVI data and their temporal and spatial patterns were explored on the Tibetan Plateau (TP). The results showed that the start of season (SOS) has significantly earlier trend in the first decade, while the end of season (EOS) has slightly (not significant) earlier trend. In the spatial dimension, similar patterns were also identified. The SOS plays a more significant role in regulating vegetation growing season length than EOS does. The EOS and driving effects from each factor exhibited spatially heterogeneous patterns. Biological factor is the dominant factor regulating the spatial pattern of EOS, while climate factors control its inter-annual variation.

1. Introduction

Vegetation phenology is finely tuned to environments and has a close relationship with climates (de Jong et al., 2011; Garonna et al., 2016). Shifts in phenology also affect feedbacks of vegetation to climate by influencing regional to global carbon budgets, fluxes of water, and energy balance (Ganguly et al., 2010; Richardson et al., 2013; Wang et al., 2017). Previous phenology studies have been mainly focused on start of season (SOS) and some showed earlier spring extended growing season length over the past three decades (Park et al., 2016; Piao et al., 2007; Wang et al., 2017). The end of season (EOS) can play an equally important role in determining growing season length, while its changes remain less studied. The reason might lie in that autumn phenology is controlled by a complexity of environmental and biological factors (Barichivich et al., 2013; Liu et al., 2016; Way and Montgomery, 2015). Researches on EOS changes are essential to improve autumn phenology models and enrich our understanding on carbon cycles in the context of ongoing global climate changes.

Remote sensing can deliver valuable information in monitoring vegetation dynamics of a variety of ecosystems, including grasslands, forests and croplands (Gonsamo and Chen, 2016; Zhao et al., 2015). Phenology analysis facilitated by remote sensing-based NDVI data have

been conducted at various spatial scales (Butt et al., 2011; Fu et al., 2014a; Jeong et al., 2011). Vegetation phenology exerts significant effects on ecosystem productivity (Dragoni et al., 2011; Duveneck and Thompson, 2017; Schwartz et al., 2006; Wu et al., 2013). It has been suggested that earlier trend of spring phenology enhances vegetation activity and increases spring carbon uptake (Wang et al., 2017; Wolf et al., 2016), while warming autumn offset parts of increased spring carbon dioxide uptake by stronger ecosystem respiration (Piao et al., 2008). Meanwhile, extended growing season length is positively correlated with GPP and NPP (Kang et al., 2016; Piao et al., 2007). Clearly, growing season length is influenced by SOS and EOS, while their relative contribution to the growing season length varies geographically. In the Northern Hemisphere, the EOS variations are greater than those of SOS. It indicates that lengthened growing season was mainly attributed to EOS (Garonna et al., 2014; Tang et al., 2015b). While at the circumpolar scale, contributions of autumn phenology to growing season length are stronger than those of spring phenology (Park et al., 2016; Zhao et al., 2015). In view of these scenarios and their varying contributions to carbon cycling, knowledge on the relative role played by SOS and EOS is essential to climate change research.

Compared with SOS, variations of EOS and its driving factors are more elusive (Che et al., 2014; Gallinat et al., 2015). Previous studies

* Corresponding author at: Key Laboratory of Ecosystem Network Observation and Modeling, Institute of Geographic Sciences and Natural Resources Research, Chinese Academy of Sciences, Beijing, China.

E-mail address: zhangyj@igsrr.ac.cn (Y. Zhang).

<https://doi.org/10.1016/j.jag.2018.03.006>

Received 24 January 2018; Received in revised form 22 March 2018; Accepted 22 March 2018
0303-2434/ © 2018 Elsevier B.V. All rights reserved.

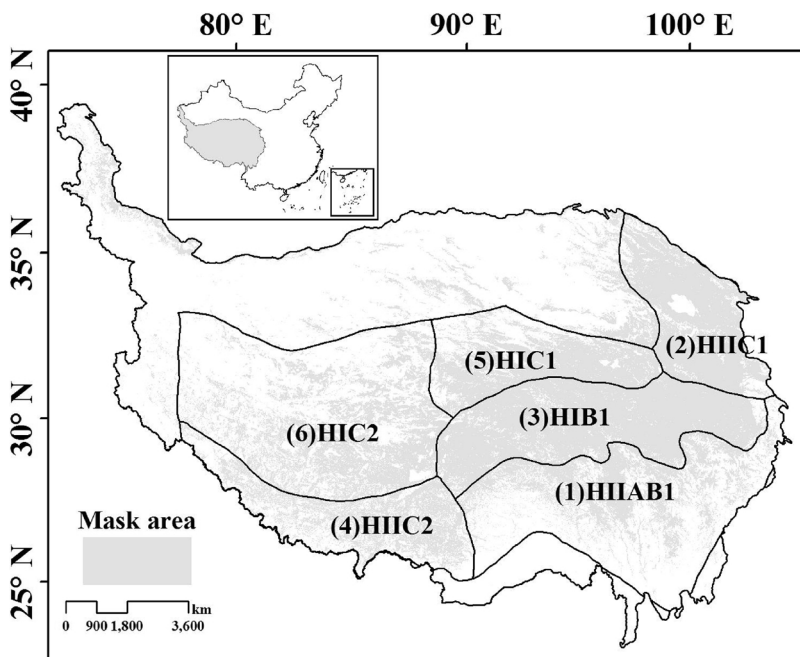


Fig. 1. Mask area and eco-regions. (1) HIIAB1: Western-Sichuan and Eastern-Tibet mountains and valleys region. (2) HII C1: Eastern Qinghai-Qilian mountains region. (3) HIB1: Guoluo-Naqui Alpine region. (4) HII C2: Southern-Tibet mountains region. (5) HIC1: Southern-Qinghai plateau valley region. (6) HIC2: Qiangtang plateau lake basin region.

have noted that warmer temperature would benefit vegetation growth and thus postpone onset of senescence (Jeong et al., 2011; Piao et al., 2006). In water constrained areas, increased temperature exacerbates moisture stress on vegetation and its limitation effects (Tang et al., 2015a; Yang et al., 2015). Solar radiation can also exert considerable influences on autumn vegetation activity by retarding abscisic accumulation and increasing photosynthetic active radiation (PAR), subsequently slowing leaf senescence (Kong et al., 2017; Liu et al., 2016). On the other hand, for ecosystems receiving inadequate autumn solar radiation, contribution effects of extending autumn phenology and promoting photosynthesis from other climatic factors are weakened (Richardson et al., 2010). Besides climate factors, biological factors can also affect EOS due to a fact that plant life-cycle stage depends on the previous ones. Both field experiments and model results showed that vegetation SOS regulates EOS (Cong et al., 2016; Fu et al., 2014b; Keenan and Richardson, 2015; Liu et al., 2016). The peak growth in summer, conventionally indicated by maximum NDVI, can also cause lag effects on subsequent autumn phenology (Wolf et al., 2016). Our current knowledge on the physiological mechanism of EOS is in shortage in regard to the complex interactions among these driving factors. It severely undermines our capacity in predicting growing season length.

Response of vegetation ecological processes to climate change can exhibit nonlinear (Park et al., 2015). The boosted regression trees (BRT) is a relatively new technique and can account for the non-linear processes largely (Elith et al., 2008). One advantage of the BRT model lies in its capability handling different types of predictor variables without prior data transformation or outliers elimination. Due to its high efficiency in handling a mixture of climate and other types of variables, recently the BRT has been widely applied on ecology researches (Leathwick et al., 2006; Liu et al., 2013).

The Tibetan Plateau represents an extreme environment due to its cold, dry and high altitude conditions. Over the past decades, temperature has been rising on the TP significantly and caused obvious impacts on vegetation growth (Yu et al., 2010; Zhang et al., 2013). However, our knowledge on confounded effects from physiological and biological factors on autumn phenology is still in severe shortage (Shen et al., 2015). To fill the gap, this study was aimed to investigate the temporal trends of vegetation EOS and their spatial variability on the TP, as well as the relative contributions of biological and climate

factors. Specifically, the objectives were to: 1) quantify the relative contribution of SOS and EOS to growing season length; 2) identify the main biological and climate driving forces on autumn phenology. The findings of this study would shed light on the mechanisms behind the EOS dynamics.

2. Methodology

2.1. Study area and data sources

The Tibetan Plateau is located in the southwest China, and its main part includes Qinghai and Tibet provinces. Its spatial extent spans from 25.9 to 35.8°N to 73.4 to 104.6°E, covering a total area of $2.58 \times 10^6 \text{ Km}^2$. Precipitation decreases from more than 1000 mm in southeast to 100 mm in northwest and reaches the maximum in summer, while annual mean temperature increases from lower than -8°C to 8°C from northwest to southeast. Steppe and meadow make up most of the land cover on the TP.

The MODIS NDVI dataset (MOD13A2) was utilized in extracting vegetation phenology from 2000 to 2015 (<https://ladsweb.nascom.nasa.gov/search/>). The 16-day temporal resolution data produced by MVC (Maximum Value Composite) method can eliminate noises caused by cloud, atmosphere and solar elevation angle to some extents. Daily temperature and precipitation data with a spatial resolution of $0.1^\circ \times 0.1^\circ$ was provided by Cold and Arid Regions Science Data Center (<http://westdc.westgis.ac.cn>) at Lanzhou. To fit all data to the same resolution, we resampled climate data to the same resolution as MODIS data. Moreover, eco-region data is provided by Data Center for Resources and Environmental Sciences, Chinese Academy of Sciences (RESDC) (<http://www.resdc.cn>).

Considering the low accuracies of NDVI data in extracting phenology for sparsely or densely vegetated lands, only pixels meeting the following criterions were included in the further phenology analyses: 1) the maximum NDVI value occurs between July and September; 2) the maximum averaged monthly (6–9) NDVI value is no less than 0.2; 3) the average winter NDVI value is less than 0.3 (Ding et al., 2016; Shen et al., 2014). These rules can minimize the data uncertainties. Fig. 1 shows the masked area and eco-regions on the TP.

2.2. Data analysis

The Asymmetric Gaussian function in the TIMESAT program has been reported to perform well in reconstructing NDVI time series on the TP (Liu et al., 2014; Song et al., 2011). In this method, two Gaussian functions are first used to fit the left and right NDVI curves around the maxima and minima. Then a global fitting function was used to merge left and right Gaussian functions into one (Jönsson and Eklundh, 2004). Phenological parameters are usually extracted using the dynamic threshold method based on the left and right Gaussian functions. In this study, the Asymmetric Gaussian function in the TIMESAT was employed to extract the following metrics (Eklundh and Jönsson, 2015): SOS (Start of growing season), EOS (End of growing season), LOS (Length for growing season), MD (Middle season date), and MN (Maximum NDVI during growing season). The envelope iterations of 3, strength of 2, SOS threshold of 0.2 and EOS threshold of 0.7 were defined in extracting phenological stages.

The linear statistical techniques are commonly used in assessing the spatial-temporal trends of variables. However, the conventional linear model is not suitable for non-parametric data, for which non-parametric methods (Mann-Kendall test) are efficient. The Mann-Kendall trend test is a rank-based method to identify trend, and suitable for non-normal distributed time series. For a time series data, the slope was first calculated between two random points. Then the slopes are ranked from smallest to largest and the median slope was selected as the Sen's slope. The Sen's slope method is efficient in detecting changing trends due to its non-susceptibility to extreme values (Fu et al., 2016; Gocic and Trajkovic, 2013). After applying the MK test to each pixel, we calculated the relative contribution of trends in SOS and EOS to LOS via C-index of the Sen's slope as follows (Garonna et al., 2014):

$$C = -1 + \frac{2 * abs(\Delta SOS)}{abs(\Delta SOS) + abs(\Delta EOS)} \quad (1)$$

Where ΔSOS and ΔEOS are the Sen's slope of SOS and EOS, respectively. A positive C value represents the change in LOS is mostly attributable to a shift in SOS, while a negative C value indicates a shift to EOS.

We defined pre-season as the period preceding EOS (16-year-average EOS) to two months ahead. For the pre-season period, we calculated annual average temperature, total precipitation and total insolation in each pixel as climate factors. In assessing the relative importance of each factor to autumn phenology, the boosted regression tree (BRT) model was applied. The BRT model has improved performance over a single model by fitting and combining several models in prediction (Elith et al., 2008; Fang et al., 2015). We used SOS, MD, MN, pre-season temperature (Tem), precipitation (Pre), insolation (Rad) as predictor variables, and set EOS as a response variable in the BRT model. The following parameters were set when fitting regression trees: tree complexity = 5, learning rate = 0.005 and bag fraction = 0.5. To reduce stochasticity caused by random sampling and bagging, 10 BRT models were generated for each year and their results were averaged in evaluating the relative importance of the driving variables. The relative importance associated with the same location pixel in each eco-region was also modeled to explore the drivers on inter-annual EOS changes. All the process were implemented in the R (version 3.3.2) software supported by "gbm" and "dismo" packages.

3. Results

3.1. Temporal variations of phenological metrics on the TP

Overall, the spring phenology exhibited an earlier trend with a Sen's slope of $-0.45 \text{ day yr}^{-1}$ ($p > 0.1$) over the whole plateau from 2000 to 2015 (Fig. 2a). Compared with the entire study period, the first twelve years displayed a steeper trend. The Sen's slope of autumn phenology was 0.12 and $-0.05 \text{ day yr}^{-1}$ for the first decade and the whole period, respectively, neither being significant (Fig. 2b). During

the initial period (2000–2011), the growing season length was significantly extended by 1.25 day yr^{-1} , while the opposite trend during the later period made the overall trend from 2000 to 2015 insignificant. Clearly, spring phenology was the main factor controlling the growing season length (Fig. 2c).

During 2000–2015, over 71.1% of the study area exhibited earlier trends of SOS, with approximately 25.0% of them statistically being significant (Fig. 3a). Later trends of SOS was mainly distributed in the southwest, with 7.2% of them displaying significant trends. The EOS displayed similar patterns with SOS and pixels with an earlier trend of EOS accounted for 49.4% of the total pixels mainly distributed in middle TP (Fig. 3b). Positive EOS trends mainly occurred in north-western TP, eastern region of Qinghai Lake and scattered sporadically in the middle-east TP. Extended LOS were mainly concentrated in eastern TP, with 17.4% of pixels showing significant trends. Shortened LOS mainly occurred in southwestern TP, with 11.4% exhibiting significant trend (Fig. 3c). As shown in Fig. 3d, more than half of the study area indicated positive C-index value (30.6% of pixels significant), which represents the greater contribution to the LOS from SOS than from EOS. Pixels with the C-index value over 0.4 were mainly distributed in the middle and north TP. The negative C-index value indicates the stronger EOS trend than SOS and its spatial pattern were similar with shortened LOS (Fig. 3c).

3.2. Drivers on spatial-temporal dynamics of autumn phenology

The relative importance showed that MD and SOS ranked as the two most important variables (determining 79.5% variations) in determining the spatial pattern of EOS (Fig. 4a). The relative importance value for SOS is significantly less than MD. The remaining four variables together accounted for 20.5% of the relative importance, with a ranking of Rad > MN > Tem > Pre. Though Rad only accounted for 14.6% of the total variations, it is the most important climate variable compared with Tem and Pre. The mean relative importance value for MN was similar to that of Tem and Pre, but showed larger variations than Tem and Pre. Based on EOS timing, five regions were divided and each region was fit a BRT model (Fig. 4b). On the whole, MD and SOS still played as the top two variables in determining EOS. The MD and SOS exhibited negative relationships with EOS and MD exerted a stronger influence. The relative importance value for Rad increased before the day of 273, then following a slightly decreasing trend, and its relative importance is greater than that of the rest three variables in each phenological segment.

The relative driving magnitude from each factor was assessed for the six eco-regions separately (Fig. 5). Specifically, in humid region, Tem, MD and Rad were the main factors controlling the inter-annual variations of EOS (Fig. 5a, b). The contribution of Pre and other phenological metrics is relatively small, accounting for less than 35% and 28%, respectively. In the central part of TP, Rad and SOS occupy the highest ranks, and the MN gradually exceeded the role played by each of the remaining variables (Fig. 5c). Impacts of Pre became prominent in southwestern TP, while effects of Rad on EOS are not significant in the abovementioned eco-regions (Fig. 5d). Furthermore, MD and SOS also played important roles, second only to Pre. Similar to other eco-regions in the middle part of TP, Rad exerted a primary effect, followed by Pre, SOS and Tem (Fig. 5e). In the western TP, the relative importance value for SOS surpassed each of the remaining variables (Fig. 5f).

We used 12 years data to construct BRT model and the remaining four years as validation. Then we randomly sampled 0.02% pixels in each year to assess their linear relationships (Fig. 6a). The actual EOS and predicted EOS displayed a good linear relationship with a correlation coefficient r of 0.86 ($p < 0.01$). In addition, almost 55% of pixels showed greater actual EOS than predicted values (Fig. 6b). The within -10 and 10 difference between actual EOS and predicted EOS accounted for about 85% of the total pixels in the four years, which is

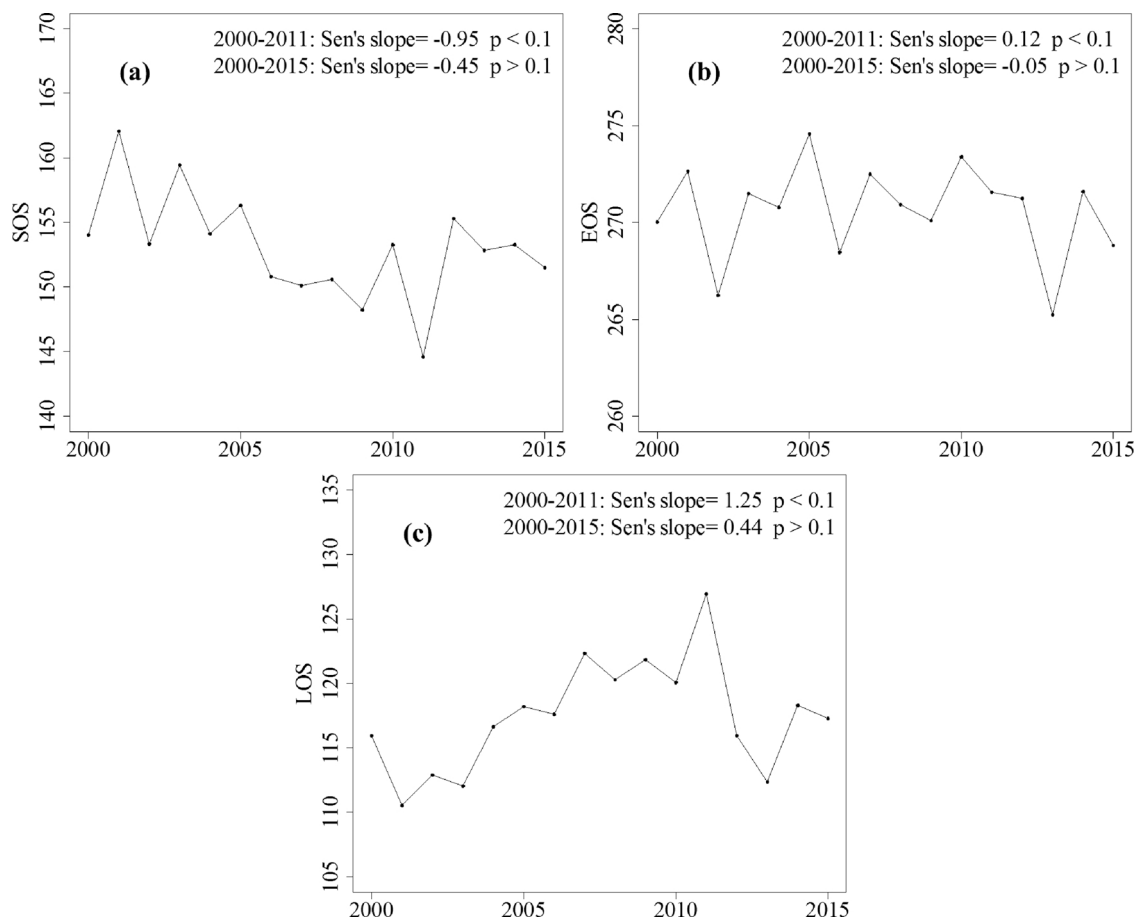


Fig. 2. Inter-annual variations of phenological metrics over the entire study period.

less than the temporal resolution of satellite data (MOD13A2). These results indicate that it is appropriate to use BRT model to analyze the spatial and temporal patterns of phenology in TP.

4. Discussion

4.1. Changes in phenology on the TP

This study revealed an overall earlier trend of SOS ($-0.45 \text{ day yr}^{-1}$), while EOS displayed a slight but non-significant advancement ($-0.05 \text{ day yr}^{-1}$) over the whole TP during the past decade. These results were not in accord with other similar studies conducted on the TP (Cong et al., 2016; Zhang et al., 2013). The discrepancies might be largely due to their different targeted periods and also based on different phenology extraction methods. The spring phenology exhibited distinct trends for the period prior to and post 2011, probably caused by shifted climate trends between the two periods (Ding et al., 2016; Sun et al., 2016).

The temporal phenology variations showed that extended growing season length (2000–2011) was mainly due to earlier trend of SOS. The spatial analysis also supported this as more than half of the study area displayed stronger contributions of SOS than EOS to extended growing season length. Most pixels with earlier trend of SOS were mainly distributed in mid-eastern TP, where probably caused by increased pre-winter and spring temperatures (Zhang et al., 2013). Similar studies conducted for North America and Europe showed that prolonged growing season length stemmed mainly from variations of EOS (Garonna et al., 2014; Zhu et al., 2012), caused by a strong autumn temperature increase in most parts of Northern Hemisphere from 1982 to 2013 (Kong et al., 2017). Extended growing season has high

ecological significance to ecosystem productivity. It is generally agreed that prolonged growing season resulted in stronger NPP on the TP (Ding et al., 2013; Wang et al., 2017; Zhang et al., 2013). The longer availability of green plants caused by prolonged growing season can support more livestock, hereby implying high significance to agriculture and animal husbandry on the TP.

4.2. Mechanisms behind spatial and temporal patterns of EOS

Of the possible driving factors, the middle season date explained up to 55% of spatial variations in EOS, followed by SOS. The vegetation middle season date showed no significant changes over 2000–2015 on the TP (Fig. 7). Therefore, the slight fluctuation for time interval between middle season date and autumn phenology was a fix circadian rhythm of vegetation and it can be explained by phenotypic plasticity of individuals and their adaption to environments to a large extent (DeWitt et al., 1998; Farre, 2012; McWatters and Devlin, 2011; Sultan, 2000). The circadian rhythm exhibits varied sensitivity to environmental changes, as reflected by distinct survival strategies of vegetation. Under improved hydrothermal condition, autumn vegetation phenology showed a gradually later trend. This could be the vegetation resistance to environmental stress (Dong et al., 2014; Fan et al., 2007; Miklos and Rubin, 1996). In harsh environments where resource is limited, effects stemmed from biological factors of middle season date and SOS strengthen. It indicates that vegetation's life cycle is strongly regulated by its own rhythm to complete the life cycle and biological rhythm plays a critical role. While in favorable environmental conditions, vegetation does not need to play its own full capacity and vegetation growth is easier than in harsh environments. As a result, climate effects on EOS strengthen, while roles of biological factors

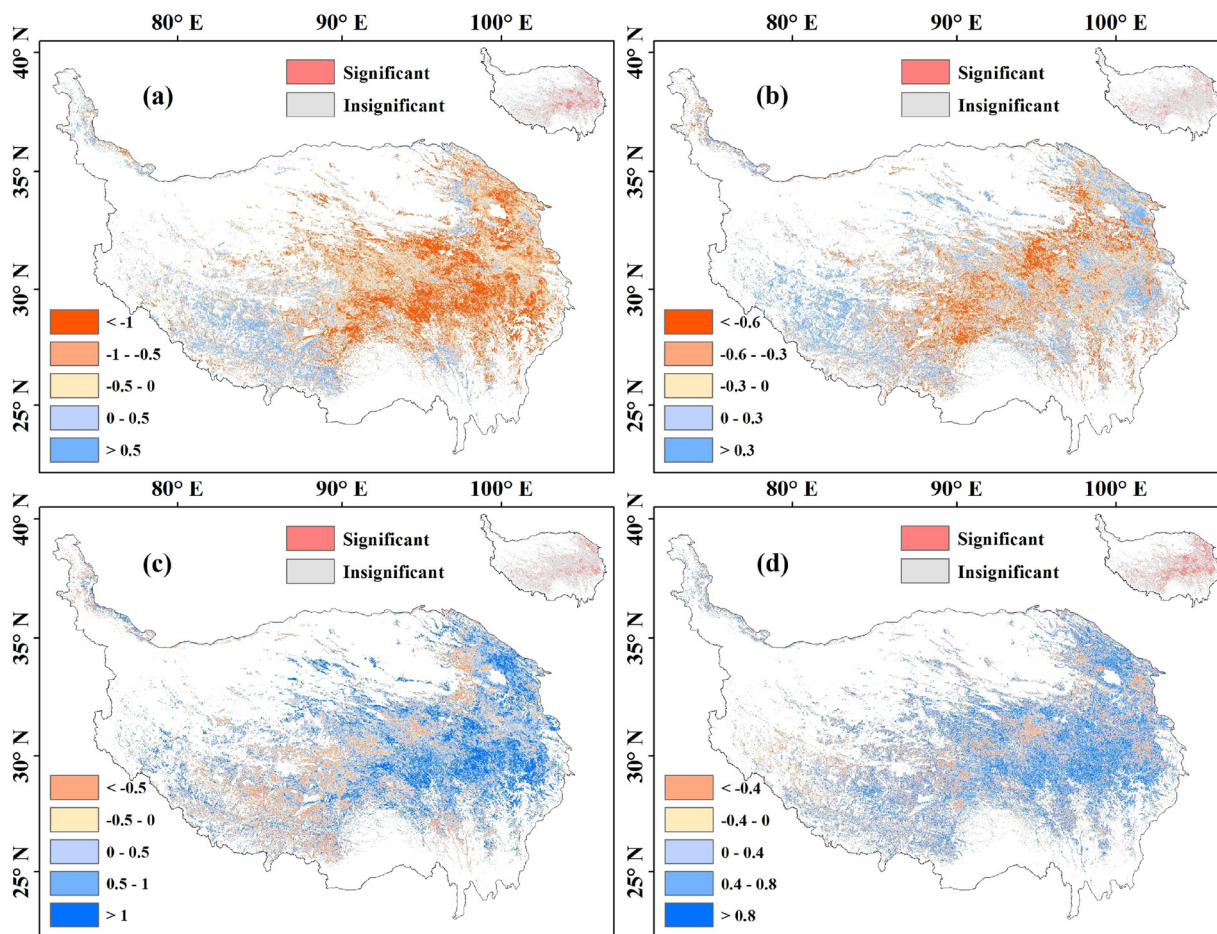


Fig. 3. Phenological change determined by the MK Sen's slope and C-index value. (a) SOS; (b) EOS; (c) LOS; (d) C-index value.

weakens.

On the TP, climate factors largely determined the inter-annual variations of autumn phenology. Specifically, the strong influence of temperature only occurred in the moisture favored eco-region HIIAB1,

indicating the boosting effects of higher temperature on vegetation growth only in wet areas (Kong et al., 2017; Zhao et al., 2015). One possible cause is that most precipitation falls in summer on the TP. Adequate water leaves lagged effects on soil moisture in autumn. Thus,

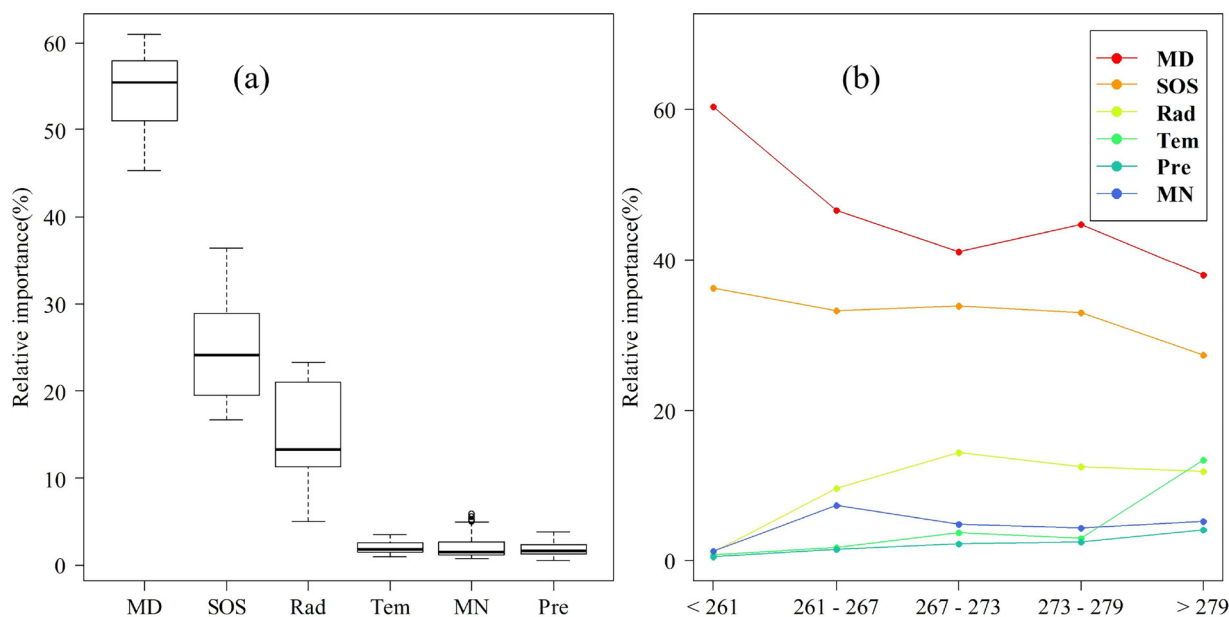


Fig. 4. (a) Relative importance proportion of variables for BRT models; (b) Relative importance proportion of variables in different EOS segments. Note: Both the left and right sub-figure use EOS as response variable in BRT model.

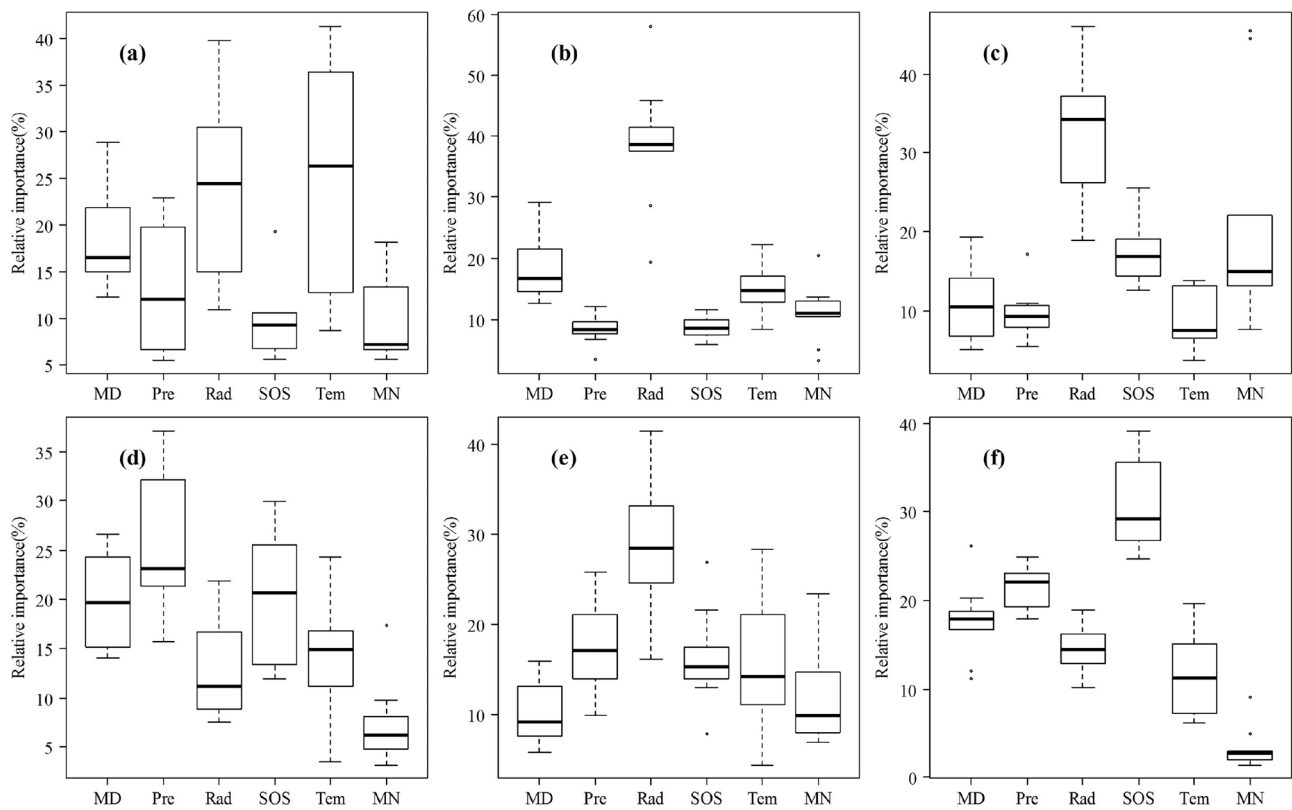


Fig. 5. The relative importance of variables based on the BRT models in 6 eco-regions. (a) eco-region HIIAB1. (b) eco-region HIIC1. (c) eco-region HIB1. (d) eco-region HIIC2. (e) eco-region HIC1. (f) eco-region HIC2. Note: Both eco-regions use EOS as response variable in the BRT model.

vegetation growth is not limited by water and temperature can promote its growth to the maximum extent (Ding et al., 2015; Zhou and Jia, 2016). While effects of temperature might be overestimated in mid-eastern TP compared with similar vegetation types in previous studies (Cong et al., 2016; Liu et al., 2016). In mid-eastern TP, solar radiation contributes most to variations in autumn phenology probably via day length (Calle et al., 2010). For example, Che et al. (2014) and Du et al. (2017) reported significant negative correlation between autumn NDVI and sunshine hours in mid-north TP, which implies that longer sunshine

duration would decrease vegetation activity and subsequently advance EOS. While some evidences also indicate that higher radiation can slow down accumulation of abscisic acid and thus delay leaf senescence (Gepstein and Thimann, 1980; Liu et al., 2016; Thimann and Satler, 1979). In the dry western TP (eco-region HIC2 and HIIC2), effects of solar radiation on EOS weakened. Reduced water availability influences water transport capacity and constrains leaf photosynthetic rate (Moshelion et al., 2015; Zhang et al., 2014). As a result, EOS varies mainly with precipitation and solar effects are marginal.

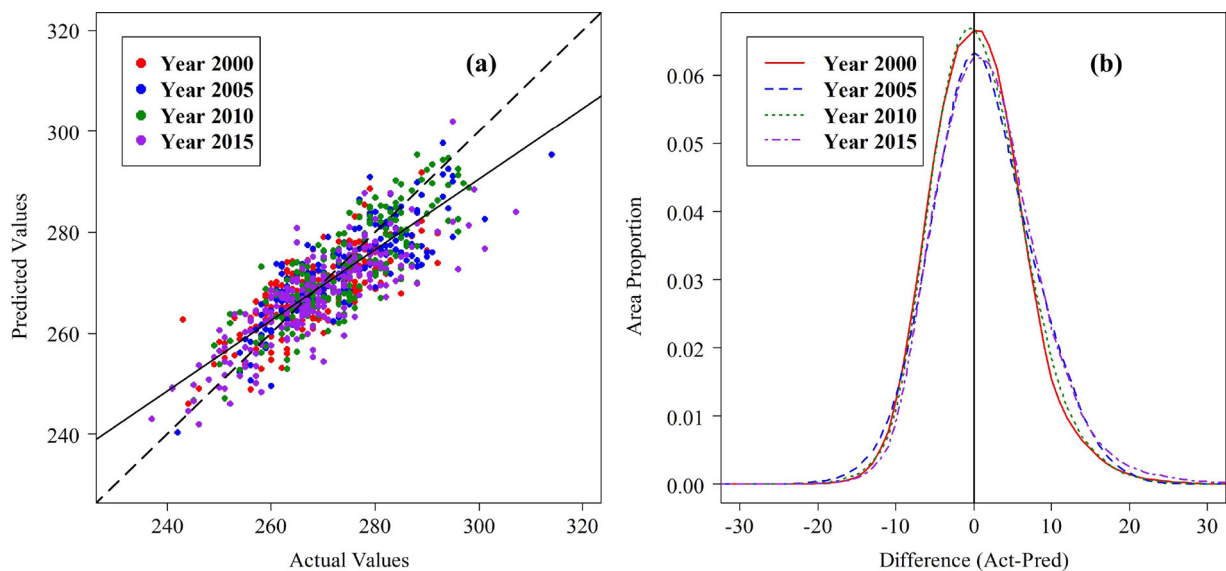


Fig. 6. (a) Scatter plots between actual EOS and predicted EOS. Solid line represents the relationship between actual EOS and predicted EOS. The dashed line is 1:1 line, which represents the relationship of actual EOS = predicted EOS. (b) The area proportion for the whole TP indicating the difference between actual EOS and predicted EOS. Note: we selected year 2000, 2005, 2010 and year 2015 to validate BRT model and the rest of years to build model.

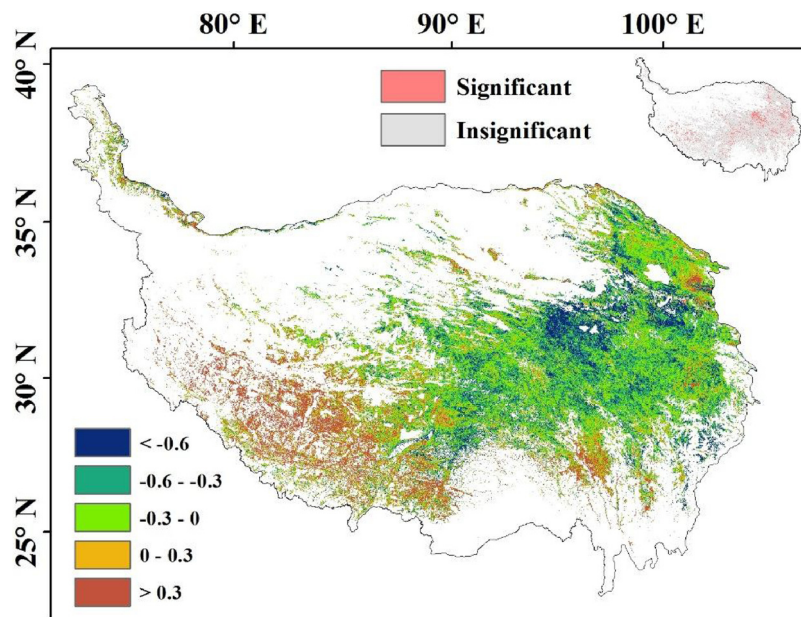


Fig. 7. The MK Sen's slope for middle season date on the Tibetan Plateau.

4.3. Evaluation of BRT model

In this study, difference between actual and predicted EOS almost evenly distributed on both sides of $x = 0$ with most values less than abs 10, which reflects the good performance of BRT model. Compared to conventional statistical models, machine learning method has brought considerable advantages (Elith et al., 2008; Rodriguez-Galiano et al., 2016). However, it should be noted that when the study area is large enough, the inside environmental heterogeneity grows. Although we tried our best to predict EOS, larger difference still exists in earlier and later EOS area. Therefore, in order to get a higher fitting effect as a whole, it would be a more preferable method to refine the study area and fit and adjust the models separately. Moreover, further studies are also needed to compare different algorithms which can optimize the simulation of ecosystem model.

5. Conclusions

This study utilized phenology as an index to evaluate climate change impacts on vegetation dynamics on the TP. Three regular phenological parameters were extracted using MODIS NDVI dataset for the period 2000–2015 to analyze their temporal-spatial dynamics. Driving factors on autumn phenology were emphatically investigated using BRT model for the whole TP and different eco-regions. The results demonstrated that earlier trend of SOS contributed mostly to extended LOS on the TP, while contribution from flat trended EOS was marginal. Furthermore, vegetation rhythm, such as middle season date and SOS, determines the spatial distribution of EOS to a large extent. For most eco-regions, effects from climate factor of solar radiation on inter-annual EOS were more obvious than vegetation's self-rhythm.

Acknowledgments

This work was supported by the International Partnership Program of Chinese Academy of Sciences (131C11KYSB20160061), Optimized Allocation System and Model of Grassland Ecology and Production in Tibetan Plateau (2016YFC0502001) and National Natural Science Foundation of China (41501103).

References

- Barichivich, J., Briffa, K.R., Myneni, R.B., Osborn, T.J., Melvin, T.M., Ciais, P., Piao, S., Tucker, C., 2013. Large-scale variations in the vegetation growing season and annual cycle of atmospheric CO₂ at high northern latitudes from 1950 to 2011. *Glob. Chang Biol.* 19, 3167–3183.
- Butt, B., Turner, M.D., Singh, A., Brottem, L., 2011. Use of MODIS NDVI to evaluate changing latitudinal gradients of rangeland phenology in Sudano-Sahelian West Africa. *Remote Sens. Environ.* 115, 3367–3376.
- Calle, Z., Schlumpberger, B.O., Piedrahita, L., Leftin, A., Hammer, S.A., Tye, A., Borchert, R., 2010. Seasonal variation in daily insolation induces synchronous bud break and flowering in the tropics. *Trees-Struct. Funct.* 24, 865–877.
- Che, M., Chen, B., Innes, J.L., Wang, G., Dou, X., Zhou, T., Zhang, H., Yan, J., Xu, G., Zhao, H., 2014. Spatial and temporal variations in the end date of the vegetation growing season throughout the Qinghai–Tibetan Plateau from 1982 to 2011. *Agric. Forest Meteorol.* 189–190, 81–90.
- Cong, N., Shen, M., Piao, S., 2016. Spatial variations in responses of vegetation autumn phenology to climate change on the Tibetan Plateau. *J. Plant Ecol.* rtw084.
- de Jong, R., de Bruin, S., de Wit, A., Schaepman, M.E., Dent, D.L., 2011. Analysis of monotonic greening and browning trends from global NDVI time-series. *Remote Sens. Environ.* 115, 692–702.
- DeWitt, T.J., Sih, A., Wilson, D.S., 1998. Costs and limits of phenotypic plasticity. *Trends Ecol. Evol.* 13, 77–81.
- Ding, M.J., Zhang, Y.L., Sun, X.M., Liu, L.S., Wang, Z.F., Bai, W.Q., 2013. Spatiotemporal variation in alpine grassland phenology in the Qinghai-Tibetan Plateau from 1999 to 2009. *Chin. Sci. Bull.* 58, 396–405.
- Ding, M., Chen, Q., Li, L., Zhang, Y., Wang, Z., Liu, L., Sun, X., 2015. Temperature dependence of variations in the end of the growing season from 1982 to 2012 on the Qinghai–Tibetan Plateau. *GISci. Remote Sens.* 1–17.
- Ding, M.-j., Li, L.-h., Nie, Y., Chen, Q., Zhang, Y.-l., 2016. Spatio-temporal variation of spring phenology in Tibetan Plateau and its linkage to climate change from 1982 to 2012. *J. Mount. Sci.* 13, 83–94.
- Dong, Y., Wang, C.P., Han, X., Tang, S., Liu, S., Xia, X.L., Yin, W.L., 2014. A novel bHLH transcription factor PebHLH35 from *Populus euphratica* confers drought tolerance through regulating stomatal development, photosynthesis and growth in *Arabidopsis*. *Biochem. Biophys. Res. Commun.* 450, 453–458.
- Dragoni, D., Schmid, H.P., Wayson, C.A., Potter, H., Grimmond, C.S.B., Randolph, J.C., 2011. Evidence of increased net ecosystem productivity associated with a longer vegetated season in a deciduous forest in south-central Indiana, USA. *Global Change Biol.* 17, 886–897.
- Du, J., He, P., Fang, S., Liu, W., Yuan, X., Yin, J., 2017. Autumn NDVI contributes more and more to vegetation improvement in the growing season across the Tibetan Plateau. *Int. J. Digital Earth* 10, 1098–1117.
- Duveneck, M.J., Thompson, J.R., 2017. Climate change imposes phenological trade-offs on forest net primary productivity. *J. Geophys. Res.-Biogeosci.* 122, 2298–2313.
- Eklundh, L., Jönsson, P., 2015. TIMESAT32 Software Manual.
- Elith, J., Leathwick, J.R., Hastie, T., 2008. A working guide to boosted regression trees. *J. Anim. Ecol.* 77, 802–813.
- Fan, Y., Lingfeng, M., Xiao, X.U., Chunyang, L.I., 2007. Progress in research of plant responses to drought stress. *Chin. J. Appl. Environ. Biol.* 13, 586–591.
- Fang, L., Yang, J., Zu, J., Li, G., Zhang, J., 2015. Quantifying influences and relative importance of fire weather, topography, and vegetation on fire size and fire severity in a Chinese boreal forest landscape. *For. Ecol. Manage.* 356, 2–12.

- Farre, E.M., 2012. The regulation of plant growth by the circadian clock. *Plant Biol.* 14, 401–410.
- Fu, Y.H., Piao, S., Zhao, H., Jeong, S.J., Wang, X., Vitasse, Y., Ciais, P., Janssens, I.A., 2014a. Unexpected role of winter precipitation in determining heat requirement for spring vegetation green-up at northern middle and high latitudes. *Glob. Chang Biol.* 20, 3743–3755.
- Fu, Y.S.H., Campioli, M., Vitasse, Y., De Boeck, H.J., Van den Berge, J., AbdElgawad, H., Asard, H., Piao, S.L., Deckmyn, G., Janssens, I.A., 2014b. Variation in leaf flushing date influences autumnal senescence and next year's flushing date in two temperate tree species. *Proc. Natl. Acad. Sci. U. S. A.* 111, 7355–7360.
- Fu, Y., Zhao, J., Zhang, H., He, H., Guo, X., 2016. Spatiotemporal variation of vegetation phenology in the Daxing'an Mountains stratified by eco-geographical regions. *Chin. J. Appl. Ecol.* 27, 2797–2806.
- Gallinat, A.S., Primack, R.B., Wagner, D.L., 2015. Autumn, the neglected season in climate change research. *Trends Ecol. Evol.* 30, 169–176.
- Ganguly, S., Friedl, M.A., Tan, B., Zhang, X., Verma, M., 2010. Land surface phenology from MODIS: characterization of the collection 5 global land cover dynamics product. *Remote Sens. Environ.* 114, 1805–1816.
- Garonna, I., de Jong, R., de Wit, A.J., Mucher, C.A., Schmid, B., Schaepman, M.E., 2014. Strong contribution of autumn phenology to changes in satellite-derived growing season length estimates across Europe (1982–2011). *Glob. Chang Biol.* 20, 3457–3470.
- Garonna, I., de Jong, R., Schaepman, M.E., 2016. Variability and evolution of global land surface phenology over the past three decades (1982–2012). *Glob. Chang Biol.* 22, 1456–1468.
- Gepstein, S., Thimann, K.V., 1980. Changes in the abscisic acid content of oat leaves during senescence. *Proc. Natl. Acad. Sci. U. S. A.* 77, 2050–2053.
- Gocic, M., Trajkovic, S., 2013. Analysis of changes in meteorological variables using Mann-Kendall and Sen's slope estimator statistical tests in Serbia. *Global Planet. Change* 100, 172–182.
- Gonsamo, A., Chen, J.M., 2016. Circumpolar vegetation dynamics product for global change study. *Remote Sens. Environ.* 182, 13–26.
- Jönsson, P., Eklundh, L., 2004. TIMESAT—a program for analyzing time-series of satellite sensor data. *Comput. Geosci.* 30, 833–845.
- Jeong, S.-J., Ho, C.-H., Gim, H.-J., Brown, M.E., 2011. Phenology shifts at start vs. end of growing season in temperate vegetation over the Northern Hemisphere for the period 1982–2008. *Global Change Biol.* 17, 2385–2399.
- Kang, X., Hao, Y., Cui, X., Chen, H., Huang, S., Du, Y., Li, W., Kardol, P., Xiao, X., Cui, L., 2016. Variability and changes in climate, phenology, and gross primary production of an alpine wetland ecosystem. *Remote Sens.* 8, 391.
- Keenan, T.F., Richardson, A.D., 2015. The timing of autumn senescence is affected by the timing of spring phenology: implications for predictive models. *Glob. Change Biol.* 21 (7), 2634–2641.
- Kong, D.D., Zhang, Q., Singh, V.P., Shi, P.J., 2017. Seasonal vegetation response to climate change in the Northern Hemisphere (1982–2013). *Global Planet. Change* 148, 1–8.
- Leathwick, J.R., Elith, J., Francis, M.P., Hastie, T., Taylor, P., 2006. Variation in demersal fish species richness in the oceans surrounding New Zealand: an analysis using boosted regression trees. *Mar. Ecol.-Prog. Ser.* 321, 267–281.
- Liu, Z., Yang, J., He, H.S., 2013. Identifying the threshold of dominant controls on fire spread in a boreal forest landscape of Northeast China. *PLoS One* 8, e55618.
- Liu, S., Zhang, L., Wang, C., Yan, M., Zhou, Y., Lu, L., 2014. Vegetation phenology in the tibetan plateau using MODIS data from 2000 to 2010. *Remote Sens. Inform.* 29, 25–30.
- Liu, Q., Fu, Y.H., Zhu, Z., Liu, Y., Liu, Z., Huang, M., Janssens, I.A., Piao, S., 2016. Delayed autumn phenology in the Northern Hemisphere is related to change in both climate and spring phenology. *Glob. Change Biol.* 22 (11), 3702–3711.
- McWatters, H.G., Devlin, P.F., 2011. Timing in plants—a rhythmic arrangement. *FEBS Lett.* 585, 1474–1484.
- Miklos, G.L.G., Rubin, G.M., 1996. The role of the genome project in determining gene function: insights from model organisms. *Cell* 86, 521–529.
- Moshelion, M., Halperin, O., Wallach, R., Oren, R., Way, D.A., 2015. Role of aquaporins in determining transpiration and photosynthesis in water-stressed plants: crop water-use efficiency growth and yield. *Plant Cell Environ.* 38, 1785–1793.
- Park, H., Jeong, S.-J., Ho, C.-H., Kim, J., Brown, M.E., Schaepman, M.E., 2015. Nonlinear response of vegetation green-up to local temperature variations in temperate and boreal forests in the Northern Hemisphere. *Remote Sens. Environ.* 165, 100–108.
- Park, T., Ganguly, S., Tommervik, H., Euskirchen, E.S., Høgdal, K.-A., Karlsen, S.R., Brovkin, V., Nemani, R.R., Myneni, R.B., 2016. Changes in growing season duration and productivity of northern vegetation inferred from long-term remote sensing data. *Environ. Res. Lett.* 11, 084001.
- Piao, S., Fang, J., Zhou, L., Ciais, P., Zhu, B., 2006. Variations in satellite-derived phenology in China's temperate vegetation. *Global Change Biol.* 12, 672–685.
- Piao, S., Friedlingstein, P., Ciais, P., Viovy, N., Demarty, J., 2007. Growing season extension and its impact on terrestrial carbon cycle in the Northern Hemisphere over the past two decades. *Global Biogeochem. Cycles* 21 (n/a-n/a).
- Piao, S., Ciais, P., Friedlingstein, P., Peylin, P., Reichstein, M., Luysaert, S., Margolis, H., Fang, J., Barr, A., Chen, A., Grelle, A., Hollinger, D.Y., Laurila, T., Lindroth, A., Richardson, A.D., Vesala, T., 2008. Net carbon dioxide losses of northern ecosystems in response to autumn warming. *Nature* 451, 49–52.
- Richardson, A.D., Black, T.A., Ciais, P., Delbart, N., Friedl, M.A., Gobron, N., Hollinger, D.Y., Kutsch, W.L., Longdoz, B., Luysaert, S., Migliavacca, M., Montagnani, L., Munger, J.W., Moors, E., Piao, S., Rebmann, C., Reichstein, M., Saigusa, N., Tomelleri, E., Vargas, R., Varlagin, A., 2010. Influence of spring and autumn phenological transitions on forest ecosystem productivity. *Philos. Trans. R. Soc. Lond. Ser. B, Biol. Sci.* 365, 3227–3246.
- Richardson, A.D., Keenan, T.F., Migliavacca, M., Ryu, Y., Sonnentag, O., Toomey, M., 2013. Climate change, phenology, and phenological control of vegetation feedbacks to the climate system. *Agric. Forest Meteorol.* 169, 156–173.
- Rodriguez-Galiano, V.F., Sanchez-Castillo, M., Dash, J., Atkinson, P.M., Ojeda-Zujar, J., 2016. Modelling interannual variation in the spring and autumn land surface phenology of the European forest. *Biogeosciences* 13, 3305–3317.
- Schwartz, M.D., Ahas, R., Aasa, A., 2006. Onset of spring starting earlier across the Northern Hemisphere. *Global Change Biol.* 12, 343–351.
- Shen, M., Zhang, G., Cong, N., Wang, S., Kong, W., Piao, S., 2014. Increasing altitudinal gradient of spring vegetation phenology during the last decade on the Qinghai-Tibetan Plateau. *Agric. Forest Meteorol.* 189–190, 71–80.
- Shen, M., Piao, S., Dorji, T., Liu, Q., Cong, N., Chen, X., An, S., Wang, S., Wang, T., Zhang, G., 2015. Plant phenological responses to climate change on the Tibetan Plateau: research status and challenges. *Natl. Sci. Rev.* 2, 454–467.
- Song, C., Ke, L., You, S., Liu, G., Zhong, X., 2011. Comparison of three NDVI time-series fitting methods based on TIMESAT taking the grassland in northern Tibet as case. *Remote Sens. Technol. Appl.* 26, 147–155.
- Sultan, S.E., 2000. Phenotypic plasticity for plant development, function and life history. *Trends Plant Sci.* 5, 537–542.
- Sun, J., Qin, X., Yang, J., 2016. The response of vegetation dynamics of the different alpine grassland types to temperature and precipitation on the Tibetan Plateau. *Environ. Monit. Assess.* 188, 20.
- Tang, G., Arnone Iii, J.A., Verburg, P.S.J., Jasoni, R.L., Sun, L., 2015a. Trends and climatic sensitivities of vegetation phenology in semiarid and arid ecosystems in the US Great Basin during 1982–2011. *Biogeosciences* 12, 6985–6997.
- Tang, H., Li, Z., Zhu, Z., Chen, B., Zhang, B., Xin, X., 2015b. Variability and climate change trend in vegetation phenology of recent decades in the Greater Khingan Mountain area, Northeastern China. *Remote Sens.* 7, 11914–11932.
- Thimann, K.V., Satler, S.O., 1979. Relation between leaf senescence and stomatal closure – senescence in light. *Proc. Natl. Acad. Sci. U. S. A.* 76, 2295–2298.
- Wang, S., Zhang, B., Yang, Q., Chen, G., Yang, B., Lu, L., Shen, M., Peng, Y., 2017. Responses of net primary productivity to phenological dynamics in the Tibetan Plateau, China. *Agric. Forest Meteorol.* 232, 235–246.
- Way, D.A., Montgomery, R.A., 2015. Photoperiod constraints on tree phenology, performance and migration in a warming world. *Plant Cell Environ.* 38, 1725–1736.
- Wolf, S., Keenan, T.F., Fisher, J.B., Baldocchi, D.D., Desai, A.R., Richardson, A.D., Scott, R.L., Law, B.E., Litvak, M.E., Brunzell, N.A., Peters, W., van der Laan-Luijckx, I.T., 2016. Warm spring reduced carbon cycle impact of the 2012 US summer drought. *Proc. Natl. Acad. Sci. U. S. A.* 113, 5880–5885.
- Wu, C., Gough, C.M., Chen, J.M., Gonsamo, A., 2013. Evidence of autumn phenology control on annual net ecosystem productivity in two temperate deciduous forests. *Ecol. Eng.* 60, 88–95.
- Yang, Y., Guan, H., Shen, M., Liang, W., Jiang, L., 2015. Changes in autumn vegetation dormancy onset date and the climate controls across temperate ecosystems in China from 1982 to 2010. *Glob. Chang Biol.* 21, 652–665.
- Yu, H., Luedeling, E., Xu, J., 2010. Winter and spring warming result in delayed spring phenology on the Tibetan Plateau. *Proc. Natl. Acad. Sci. U. S. A.* 107, 22151–22156.
- Zhang, G., Zhang, Y., Dong, J., Xiao, X., 2013. Green-up dates in the Tibetan Plateau have continuously advanced from 1982 to 2011. *Proc. Natl. Acad. Sci. U. S. A.* 110, 4309–4314.
- Zhang, S.-B., Sun, M., Cao, K.-F., Hu, H., Zhang, J.-L., 2014. Leaf photosynthetic rate of tropical ferns is evolutionarily linked to water transport capacity. *PLoS One* 9, e84682.
- Zhao, J., Zhang, H., Zhang, Z., Guo, X., Li, X., Chen, C., 2015. Spatial and temporal changes in vegetation phenology at middle and high latitudes of the northern Hemisphere over the past three decades. *Remote Sens.* 7, 10973–10995.
- Zhou, Y.-Z., Jia, G.-S., 2016. Precipitation as a control of vegetation phenology for temperate steppes in China. *Atmos. Ocean Sci. Lett.* 9, 162–168.
- Zhu, W., Tian, H., Xu, X., Pan, Y., Chen, G., Lin, W., 2012. Extension of the growing season due to delayed autumn over mid and high latitudes in North America during 1982–2006. *Global Ecol. Biogeogr.* 21, 260–271.